Journal of the Optical Society of Korea
Vol. 18, No. 4, August 2014, pp. 414-418

ISSN: 1226-4776(Print) / ISSN: 2093-6885(Online)
DOI: http://dx.doi.org/10.3807/JOSK.2014.18.4.414

Position Detection of a Scattering 3D Object by Use of the Axially Distributed Image Sensing Technique

Myungjin Cho[1]*, Donghak Shin[2], and Joon-Jae Lee[3]

[1]Department of Electrical, Electronic, and Control Engineering, IITC, Hankyong National University, Ansung 456-749, Korea
[2]Institute of Ambient Intelligence, Dongseo University, Busan 617-716, Korea
[3]Department of Game Mobile Contents, Keimyung University, Daegu 705-701, Korea

(Received May 19, 2014 : revised July 8, 2014 : accepted July 8, 2014)

In this paper, we present a method to detect the position of a 3D object in scattering media by using the axially distributed sensing (ADS) method. Due to the scattering noise of the elemental images recorded by the ADS method, we apply a statistical image processing algorithm where the scattering elemental images are converted into scatter-reduced ones. With the scatter-reduced elemental images, we reconstruct the 3D images using the digital reconstruction algorithm based on ray back-projection. The reconstructed images are used for the position detection of a 3D object in the scattering medium. We perform the preliminary experiments and present experimental results.

Keywords : Axially distributed image sensing, Three-dimensional detection, Scattering medium
OCIS codes : (110.0110) Imaging systems; (110.6880) Three-dimensional image acquisition

I. INTRODUCTION

Visualization and detection of a 3D object in optically scattering media is a challenging problem. An improved visualization method of scattered images can be applied to various applications such as imaging in fog, underwater, security, and medical diagnostics [1-7]. Some 3D multiperspective approaches including integral imaging and axially distributed sensing (ADS) have been studied for visualizing objects in the scattering media [8-9]. Among them, the ADS scheme can provide simple recording architecture by translating a camera along its optical axis. The recorded high-resolution elemental images generate the clear 3D plane images for the partially occluded 3D objects.

In this paper, we present a position detection method for a 3D object in scattering media by using the ADS method [10-12]. In the proposed method, we introduce the statistical signal processing to reduce the scattering effect in elemental images and the position detection process with non-linear correlation operation is newly applied to the scattered images in ADS. The proposed method is divided into four parts: (1) pickup (2) statistical image processing (3) digital reconstruction and (4) position detection. In the pickup part using the ADS method, the camera is moved along a common optical axis and multiple longitudinal 2D images of the scene are recorded. The recorded multiple 2D images of the 3D object in the scattering media are referred to as scattering elemental images. In the second statistical processing part, to reduce the scattering effects of the recorded elemental images, a statistical image processing technique is applied to the scattering elemental images. Then, the statistically processed elemental images are used to reconstruct the 3D plane images using the digital reconstruction algorithm based on ray back-projection in the third part. In the final part, the reconstructed plane images are used for 3D object detection. To show the feasibility of the proposed method, we carry out the preliminary experiments for a scattering 3D object behind a diffuser screen as the scattering medium.

II. RECOGNITION METHOD USING ADS

2.1. Pickup Method in ADS

The pickup part of the ADS method is shown in Fig. 1. We translate a single camera along the optical axis and

*Corresponding author: mjcho@hknu.ac.kr
Color versions of one or more of the figures in this paper are available online.

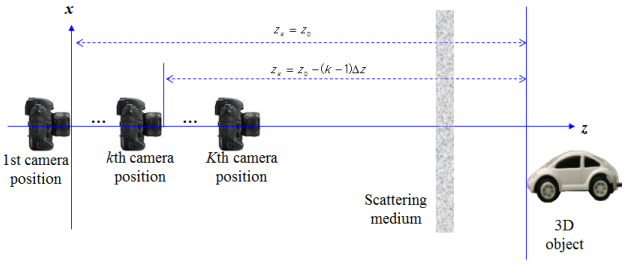

FIG. 1. Pickup part of ADS.

record multiple 2D images of the scene observed through the scattering media. We suppose that the object is located at a distance z_0 from the 1st camera position. The distance between the cameras is Δz. We record K elemental images by moving the camera. The first camera is k=1 at z_k=z_0 and the camera closest to the object becomes by k=K at z_k=z_0-(K-1)Δz. Due to the different distance from the object for each camera, the object is recorded in each elemental image with a different magnification. Each magnification ratio is calculated as M_k=z_k/g where g is the focal length of the camera.

2.2. Statistical Processing of Elemental Images

When a 3D object is located in scattering media, the recorded image may contain severe scattering noise which can prevent the correct visualization and detection for the 3D object. In this paper, therefore, we wish to reduce the noise by using statistical image processing. To do so, we apply statistical image processing techniques to the scattering elemental images. Let us assume that degradation caused by the diffuser can be modeled as Gaussian [6]. The statistical image processing procedure to reduce the scattering effect in the elemental images is shown in Fig. 2. First, we estimate the unknown parameter μ (mean) of the *Gaussian* distribution using the *Maximum Likelihood Estimation* (MLE). Here we consider that the scattering degradation function is composed of many superimposed *Gaussian* random variables with local area (w_x×w_y) of an elemental image with (N_x×N_y) pixels. Let us denote these random variables as $X_{ij}(m, n)$. Then, MLE is calculated by

$$L\left(\mu_{ij},\sigma_{ij}^2\middle|X_{ij}(m,n)\right)=\prod_{m=1}^{w_x}\prod_{n=1}^{w_y}\frac{1}{\sqrt{2\pi\sigma_{ij}^2}}e^{-\left(X_{ij}(m,n)-\mu_{ij}\right)^2/2\sigma_{ij}^2} \tag{1}$$

where $L(\cdot|\cdot)$ is the likelihood function, i=1, 2, ⋯, N_x - w_x+1, j=1, 2, ⋯, N_y - w_y+1, m=1, 2, ⋯, w_x, and n=1, 2, ⋯, w_y. And, the mean parameter $\hat{\mu}_{ij}$ of the *Gaussian* distribution is estimated as

$$\hat{\mu}_{ij}=\frac{1}{w_x w_y}\sum_{m=1}^{w_x}\sum_{n=1}^{w_y}X_{ij}(m,n) \tag{2}$$

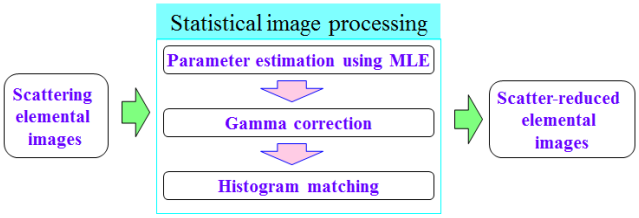

FIG. 2. Statistical image processing for the recorded elemental images.

The estimated elemental images are obtained by subtracting $\hat{\mu}_{ij}$. The estimated elemental images are given by

$$S_{ij}(m,n)=X_{ij}(m,n)-\hat{\mu}_{ij} \tag{3}$$

This estimation process enables us to reduce the scattering noise in the elemental images. *Gamma* (γ) correction is then used for the estimated elemental images. Using *Gamma* correction, we can manipulate the histogram to improve the contrast ratio [8]. Gamma correction is a non-linear method to control the overall luminance of a still image. Gamma correction is typically used to adjust still images for accurate reproduction on physical displays. In this case, it is used to compensate for the non-linear relationship between pixel values and the intensity being displayed. Therefore, for the estimated elemental images, it may be expressed by the following power-law relationship:

$$S_{corrected}=S_{uncorrected}^{\gamma} \tag{4}$$

where $S_{uncorrected}$ and $S_{corrected}$ are the uncorrected and corrected elemental images respectively, and γ is the gamma value.

Next, we apply histogram equalization and matching to the corrected elemental images. This process can remove artificial gray levels from the elemental images. We first calculate a cumulative distribution function (CDF) and this is given by

$$h_e=T(h)=\int_0^h p_h(w)dw \tag{5}$$

$$G(q)=\int_0^q p_q(t)dt=h_e \tag{6}$$

where h, h_e, and q are continuous gray levels of the histogram stretched image, the histogram equalized image, and histogram matched image. $p_h(w)$ and $p_q(t)$ are the continuous probability density functions corresponding to the h's and q, and w and t are the integration variables. Equations (5) and (6) should be followed by $G(q)$ = $T(h)$ where the inverse of the G operation yields the restored image. Finally, we can obtain the new scatter-reduced elemental images.

2.3. Digital Reconstruction in ADS

In the proposed method, the third part is the digital reconstruction using the scatter-reduced elemental images. This is shown in Fig. 3. It is based on ray back-propagation through virtual pinholes. This reconstruction algorithm numerically implements the reverse of the pickup process. In other words, all scatter-reduced elemental images are back projected and magnified by different magnifications $M_k(z)$ if the reconstruction plane is located at z. The magnified scatter-reduced elemental images are superimposed at the same reconstruction plane. Finally, we can obtain the reconstructed plane image at distance z. Then, the reconstructed plane image $r(x, y, z)$ is the summation of all the magnified elemental images S_k and is given by

$$r(x,y,z)=\frac{1}{K}\sum_{k=1}^{K}S_k\left(\frac{x}{M_k(z)},\frac{y}{M_k(z)}\right) \tag{7}$$

For faster calculation, the reconstruction process may be normalized by the magnification ratio M_1. This becomes

$$r_{normalized}(x,y,z)=\frac{1}{K}\sum_{k=1}^{K}S_k\left(\frac{x}{M_k(z)/M_1(z)},\frac{y}{M_k(z)/M_1(z)}\right) \tag{8}$$

2.4. Position Detection Process

In the last part of the proposed method, the plane image $r(x, y, z)$ reconstructed at z distance from the digital reconstruction part is used for 3D object position detection. When a plane image of the target object is reconstructed at z distance, correlation is performed with the reference image f to detect the position of the 3D object. The reference image can become a clear object image without scattering medium. Then, we simply obtain the correlation peak result from nonlinear correlation operation as given by

$$f \otimes^{\alpha} r = IFT\{|F|^{\alpha}\exp(i\phi_F)\,|R|^{\alpha}\exp(i\phi_R)\} \tag{9}$$

where a is the non-linear parameter and means the strength of the applied non-linearity. In general, the choice of a depends on the type of noise and object [14]. It could vary within the range [0, 1]. F and R are the Fourier transforms of f and r, respectively. And ϕ_F and ϕ_R represent the phase angle of f and r, respectively. In Eq. (9), the correlation peak indicates the position detection performance between the reference image and the reconstructed plane image.

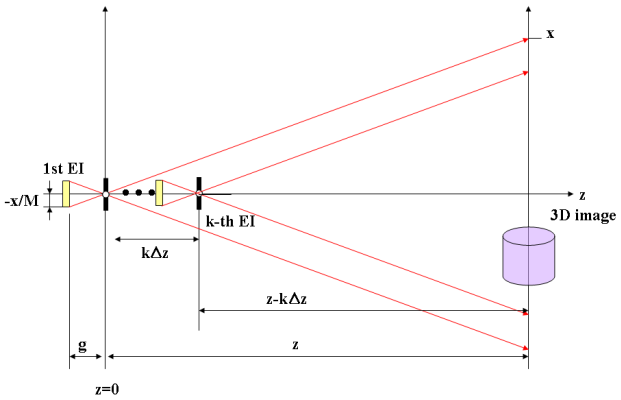

FIG. 3. Ray diagram for digital reconstruction.

III. EXPERIMENTS AND RESULTS

To demonstrate the proposed position detection method for a 3D object in scattering media, we carried out optical experiments. The experimental setup is shown in Fig. 4 where a 'car' object is positioned approximately 440 mm away from the first camera position. We placed a diffuser at approximately 50 mm in front of the object. The thickness of the diffuser was 1 mm. We used a camera with 2184× 1456 pixels with 8.2 um pixel pitch. An imaging lens with focal length g=70 mm was used. We used the camera with the smallest aperture to obtain the maximum depth of field. Then, the pinhole gap (g) becomes 70 mm in the digital reconstructions as shown in Fig. 3. The camera is moved with a step of 5 mm and a total of K=41 elemental images are recorded within a total displacement distance of 200 mm. The first elemental image and the 41st elemental image are shown in Fig. 4(c) and 4(d), respectively. We can see that the recorded elemental images were degraded by the scattering noise.

To reduce the scattering noise in the elemental images, the statistical image processing technique was applied to them as described in Fig. 3. Figure 5 shows the example of the 21st elemental image produced by the statistical image processing technique. The 21st elemental image shown in Fig. 5(a) was scatter-reduced as shown in Fig.

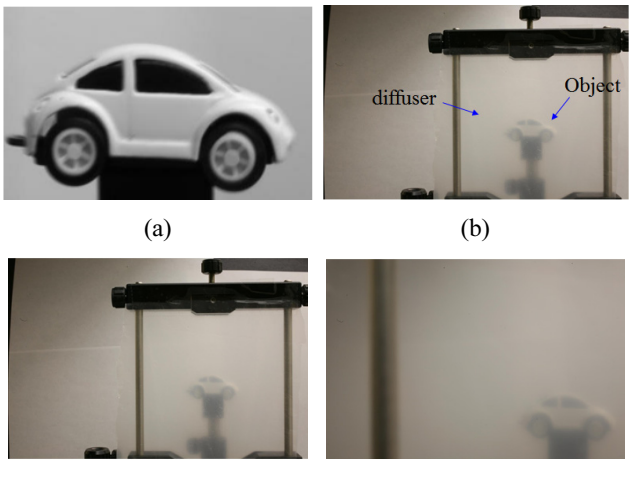

FIG. 4. (a) Original object (b) Experimental setup. (c) 1st scattering elemental image (d) 41st scattering elemental image.

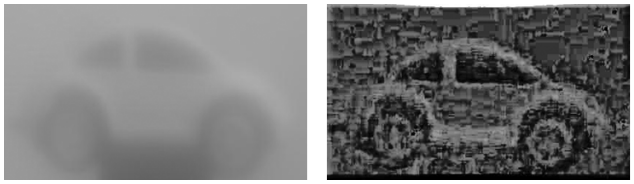

(a) (b)

FIG. 5. (a) 'car' image within 21st elemental image (b) Statistically processed images.

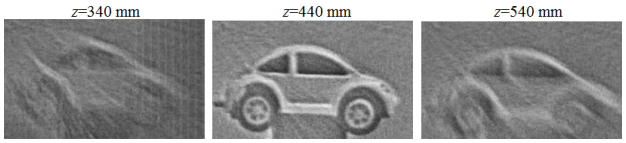

(a)

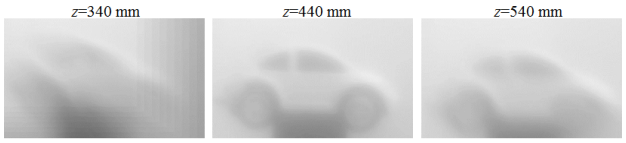

(b)

FIG. 6. Reconstructed plane images at different distances (a) Proposed method (b) Conventional method.

5(b). The statistical image processing was repeated to all the recorded elemental images. Then, we can obtain the 41 scatter-reduced elemental images.

To reconstruct the 3D images, the scatter-reduced 41 elemental images were computationally back projected through virtual pinholes according to Eq. (8). The 3D plane images were obtained according to the reconstruction distance. Some reconstructed plane images are shown in Fig. 6(a) for three different reconstruction distances (340 mm, 440 mm, and 540 mm). When the distance of reconstruction plane was 440 mm, where the 'car' object is originally located, the reconstructed image is well focused after reducing the scattering noises through the statistical image processing. For comparison, the plane images are shown in Fig. 6(b) when using the conventional method without the statistical image processing.

To detect the position of the 3D object, the non-linear correlation operation as described in Eq. (9) was used for the original reference image and the reconstructed plane images. The correlation peak results are shown in Fig. 7 according to the reconstruction distances from 340 mm to 540 mm. Here the non-linear parameter was 0.6. We can see that the correlation peaks are very low in the conventional method. This is because all of the reconstructed plane images have heavily scattered noise regardless of the reconstruction distance. On the other hand, we can see the highest correlation peak at 440 mm where the object was originally located in the result of the proposed method. At the original position of the object, the 2D correlation

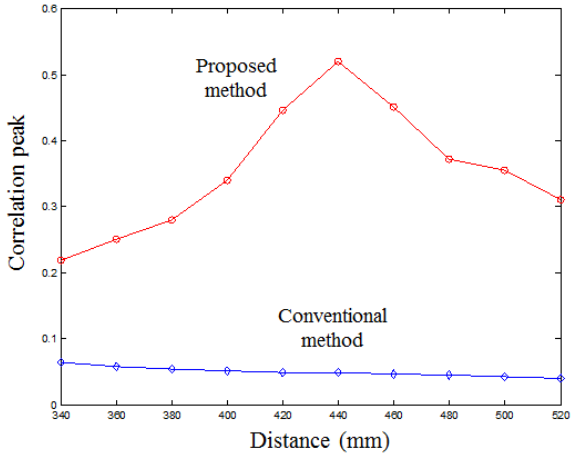

FIG. 7. Correlation peak results according to the reconstruction distance.

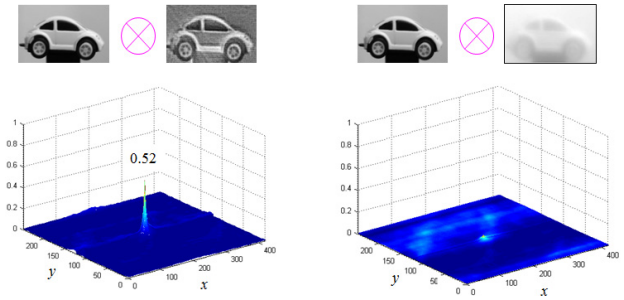

(a) (b)

FIG. 8. Non-linear correlation results when α=0.6 (a) Proposed method (b) Conventional method. x and y mean the pixel indexes of the correlation output.

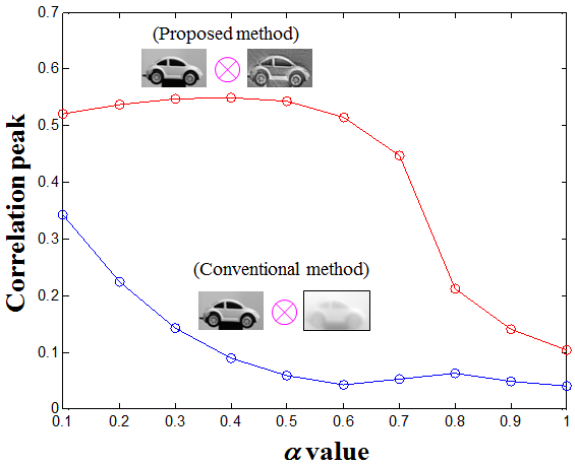

FIG. 9. Non-linear correlation results according to the α value.

output was shown in Fig. 8(a) when the original image and our scatter-reduced plane image were used. For comparison, the correlation output in the conventional method is very low when the scattered plane image was used as shown in Fig. 8(b). Figure 9 shows the graph of the maximum correlation

peaks according to the non-linear parameter (a) in Eq. (9). These results reveal that the scatter-reduced plane image provides the higher position detection performance compared with the scattered plane image for all a values.

IV. CONCLUSION

In conclusion, the ADS-based position detection method for a 3D object in scattering media was presented. The elemental images recorded by the ADS method contain severe scattering noise. To reduce the scattering noise, we applied a statistical image processing algorithm to the scattering elemental images. Thus, we were able to obtain the improved 3D plane images using the digital reconstruction algorithm based on ray back-projection. Using them, we compare the correlation performance for the proposed method and the conventional method. The experimental results reveal that the proposed method is superior to the conventional method in terms of correlation operation.

ACKNOWLEDGMENT

This research was supported in part by Basic Science Research Program through the National Research Foundation of Korea (NRF) funded by the Ministry of Education, Science and Technology (NRF-2012R1A1A2001153) and this work was supported by the IT R&D program of MKE/KEIT. [10041682, Development of high-definition 3D image processing technologies using advanced integral imaging with improved depth range].

REFERENCES

1. J. S. Tyo, M. P. Rowe, E. N. Pugh, Jr., and N. Engheta, "Target detection in optically scattering media by polarization-difference imaging," Appl. Opt. **35**, 1855-1870 (1996).
2. S. G. Narasimhan and S. K. Nayar, "Vision and the atmosphere," Int'l J. Computer Vision **48**, 233-254 (2002).
3. L. Bartolini, L. De Dominicis, M. Ferri de Collibus, G. Fornetti, M. Guarneri, E. Paglia, C. Poggi, and R. Ricci, "Underwater three-dimensional imaging with an amplitude-modulated laser radar at a 405 nm wavelength," Appl. Opt. **44**, 7130-7135 (2005).
4. T. Treibitz and Y. Y. Schechner, "Active polarization descattering," IEEE Trans. PAMI **31**, 385-399 (2009).
5. G. D. Gilbert and J. C. Pernicka, "Improvement of underwater visibility by reduction of backscatter with a circular polarization technique," Appl. Opt. **6**, 741-746 (1967).
6. M. Cho, M. Daneshpanah, I. Moon, and B. Javidi, "Three-dimensional optical sensing and visualization using integral imaging," Proc. IEEE **99**, 556-575 (2011).
7. I. Moon and B. Javidi, "Three-dimensional visualization of objects in scattering medium by use of computational integral imaging," Opt. Express **16**, 13080-13089 (2008).
8. M. Cho and B. Javidi, "Three-dimensional visualization of objects in turbid water using integral imaging," J. Display Technol. **6**, 544-547 (2010).
9. D. Shin and B. Javidi, "3D visualization of partially occluded objects using axially distributed sensing," J. Display Technol. **7**, 223-225 (2011).
10. R. Schulein, M. DaneshPanah, and B. Javidi, "3D imaging with axially distributed sensing," Opt. Lett. **34**, 2012-2014 (2009).
11. D. Shin and B. Javidi, "Three-dimensional imaging and visualization of partially occluded objects using axially distributed stereo image sensing," Opt. Lett. **37**, 1394-1396 (2012).
12. Y. Piao, M. Zhang, D. Shin, and H. Yoo, "Three-dimensional imaging and visualization using off-axially distributed image sensing," Opt. Lett. **38**, 3162-3164 (2013).
13. M. Cho and D. Shin, "3D integral imaging display using axially recorded multiple images," J. Opt. Soc. Korea **17**, 410-414 (2013).
14. B. Javidi, "Nonlinear joint power spectrum based optical correlation," Appl. Opt. **28**, 2358-2367 (1989).